Journal of Orthopaedic Translation 26 (2021) 162–170

Contents lists available at ScienceDirect

Journal of Orthopaedic Translation

journal homepage: www.journals.elsevier.com/journal-of-orthopaedic-translation

Original Article

Effect of book-shaped acellular tendon scaffold with bone marrow mesenchymal stem cells sheets on bone–tendon interface healing

Yongchun Zhou [a,c,d,e,☆], Shanshan Xie [a,d,e,☆], Yifu Tang [a,d,e], Xiaoning Li [a,d,e], Yong Cao [b,d,e], Jianzhong Hu [b,d,e,**], Hongbin Lu [a,d,e,*]

[a] Department of Sports Medicine, Xiangya Hospital, Central South University, Changsha, 410008, People's Republic of China
[b] Department of Spine Surgery, Xiangya Hospital, Central South University, Changsha, 410008, People's Republic of China
[c] Department of Orthopedic, Shaanxi Provincial People's Hospital, Xi'an, 710000, People's Republic of China
[d] Key Laboratory of Organ Injury, Aging and Regenerative Medicine of Hunan Province, People's Republic of China
[e] Xiangya Hospital-International Chinese Musculoskeletal Research Society Sports Medicine Research Centre, People's Republic of China

ARTICLE INFO

Keywords:
Bone marrow mesenchymal stem cell sheets
Book-shaped acellular tendon scaffold
Patella-patellar tendon interface
Regeneration
Tissue engineering

ABSTRACT

Background: Tissue engineering has exhibited great effect on treatment for bone-tendon interface (BTI) injury. The aim of this study was to evaluate the effect of a book-shaped acellular tendon scaffold (ATS) with bone marrow mesenchymal stem cells sheets (MSCS) for BTI injury repair.

Methods: ATS was designed based on the shape of "book", decellularization effect was evaluated by Hematoxylin and eosin (H&E), 4′, 6-diamidino-2-phenylindole (DAPI) and scanning electron microscopy (SEM), then bone marrow mesenchymal stem cells (MSCs) were cultured on ATS to assess the differentiation inductivity of ATS. A rabbit right partial patellotomy model was established, and MSCS seeded on ATS were implanted into the lesion site. The patella-patellar tendon (PPT) at 2, 4, 8 or 16 weeks post-operation were obtained for histological, biomechanical and immunofluorescence analysis.

Results: H&E, DAPI and SEM results confirmed the efficiency of decellularization of ATS, and their in vitro tenogenic and chondrogenic ability were successfully identified. In vivo results showed increased macrophage polarization toward the M2 phenotype, IL-10 expression, regenerated bone and fibrocartilage at the patella-patellar tendon interface of animals received MSCS modified ATS implantation. In addition, the level of tensile strength was also the highest in MSCS modified ATS implantation group.

Conclusion: This study suggests that ATS combined with MSCS performed therapeutic effects on promoting the regeneration of cartilage layer and enhancing the healing quality of patella-patellar tendon interface.

The translational potential of this article: This study showed the good biocompatibility of the ATS, as well as the great efficacy of ATS with MSCS on tendon to bone healing. The results meant that the novel book-shaped ATS with MSCS may have a great potential for clinical application.

Introduction

The bone–tendon interface (BTI) has a transitional structure [1,2], which can disperse stress from bone to tendon and balance the mechanical load at the interface [3,4]. BTI injury is common in exercise, such as jumping, cutting and pivoting. Unfortunately, because of the slow and difficult regeneration of the fibrocartilage layer [4–7], surgery to establish bone and tendon reattachment often has high failure rate [8–10].

In recent years, scaffolds and stem cells have been widely used in tissue engineering for the repair of tendon to bone [11–15]. However, the scaffolds used in these studies are all synthetic biomaterials, which cannot completely simulate the special tissue structure and matrix components at the BTI, and lack internal biological activity, so their application is limited to some extent. Acellular bioscaffolds have the low immunogenicity, preserved physiological structure and extracellular matrix components of the native tissue [16–18], which are important for cell proliferation and differentiation [19]. At the same time, studies have shown that bone marrow mesenchymal stem cells (MSCs) have the

* Corresponding author. Department of Sports Medicine, Xiangya Hospital, Central South University, 87# Xiang-ya Road, Changsha, Hunan, 410008, China.
** Corresponding author. Department of Spine Surgery, Xiangya Hospital, Central South University, 87# Xiang-ya Road, Changsha, Hunan, 410008, China.
E-mail addresses: jianzhonghu@hotmail.com (J. Hu), hongbinlu@hotmail.com (H. Lu).
☆ Co-first authors.

https://doi.org/10.1016/j.jot.2020.02.013
Received 27 September 2019; Received in revised form 27 February 2020; Accepted 28 February 2020
Available online 24 March 2020

potential of multidirectional differentiation into bone, cartilage and tendon under different inductive microenvironment [20–22], so seeding MSCs on certain acellular scaffolds with inductive property might be effective for patella–patellar tendon (PPT) repair.

Traditional tissue engineering techniques often use high-density cell suspension for cell planting, but this method is prone to cell loss, uneven cell distribution and lack of cells in the surrounding areas of the scaffold. Recently, cell sheet engineering characterised by abundant cells and ECM has avoided above disadvantages, which has been used for the repair of damaged tissues, such as cartilage, cornea and skin [23–25]. In addition, mesenchymal stem cells sheets (MSCSs) have been applied in the regeneration of bone, cartilage and ligament [26–28]. To better combine the cell sheets with the scaffold, we designed a novel book-shaped scaffold, which is not only convenient for operation but also easy for decellularisation and cell plant. Therefore, based on abovementioned conditions, we hypothesised that the novel acellular tendon scaffold (ATS) sandwiched with bone marrow MSCSs can promote regeneration of the fibrocartilage layer at BTI injury.

In this study, a composite containing MSCS and the book-shaped ATS was applied to the rabbit partial patellotomy model. After 2, 4, 8 or 16 weeks postoperation, the effects of the composite on the healing quality at the PPT interface were investigated.

Materials and methods

Design of book-shaped acellular tendon scaffolds

After euthanasia (intravenous injection with sodium pentobarbital, 100 mg/kg) of New Zealand white rabbits which weigh 3.0 ± 0.5 kg (18-weeks-old), samples of the tendon were collected from the Achilles tendon and trimmed into cuboid (about 7 mm × 2 mm × 2 mm).

The book-shaped ATSs were prepared as previously described [17]. Briefly, the trimmed tendon segments were frozen into sections with a thickness of 200 μm but left the end uncut using cryostat (CM1950; Leica, Nussloch, Germany), and a book-shaped tendon scaffold with five layers was achieved, which was about 7 mm × 2 mm × 1 mm. Then, the book-shaped ATS were treated with five freeze–thaw cycles, followed by sodium dodecyl sulfate (0.1%) for a slight shaking for 4 h.

Evaluation of tendon scaffolds decellularisation effect

The samples used for histological evaluation were fixed with 4% paraformaldehyde. Haematoxylin and eosin (H&E) and 4′,6-diamidino-2-phenylindole (DAPI) were used to show the collagen fibrous structure and cellular components (n = 3).

After being treated with glutaraldehyde (2.5%) for 24 h, the samples were dehydrated with gradient ethanol, soaked with osmium tetroxide, dried and sprayed, then being observed by scanning electron microscopy to analysis the microstructure (n = 3).

Isolation, culture and seeding of bone marrow MSCs

MSCs were collected from New Zealand rabbits, isolated and cultured by a previously established protocol [29]. The sterilised ATSs were soaked in complete culture medium (DMEM/F12 containing 10% foetal bovine serum and 1% penicillin/streptomycin) for 24 h before seeding. The third generation MSCs were planted into a 24-well culture plate with 100 μL each, at a concentration of 2 × 105 cells/mL, and the well with ATS placed is the experimental group. After incubating for 2 h (5% CO_2, 37°C), culture medium was added into the culture plate with 2 mL each well and continue to culture in the incubator.

***Quantitative real time - polymerase chain reaction** (qRT-PCR)*

The gene expression of tenomodulin, alpha-1 type I collagen, Sox-9 and Aggrecan were measured after co-culture for 7 and 14 days (n = 8). After digestion and centrifugation, samples of cells in each group were collected in liquid nitrogen. Then extracted mRNA from cells were resuspended in RNAase-free H_2O, then subjected to Prime-Script™ RT reagent kit (TaKaRa, Kusatsu, Japan) for synthesis of complementary DNA. SYBR Green PCR Master Mix was used for qRT-PCR. The primer sequences of genes to be tested for qRT-PCR were summarised in Table 1.

Table 1
Reverse transcription–polymerase chain reaction primer sequences.

Genes	Forward primer sequences	Reverse primer sequences
GAPDH	ATGGTGAAGGTCGGAGTGAA	GCAAACCTTCTCAAACTCGCCCAC
Sox-9	CGCCCCCGCTAGCCGCACGA	CTGGTGCTCCGCGTAGTCGAACTG
Aggrecan	CCCAACTGCGGCGGAAACCT	ATGTCCTCCTCACCGCCCACTCC
Tenomodulin	CCATGCTGGATGAGAGAGGTT	CCGTCCTCCTTGGTAGCAGT
Alpha-1 type I collagen	ATGGATTCCAGTTCGAGTAGGC	CATCGACAGTGACGCTGTAGG

Immunofluorescence

Protein expression of Sox-9 and tenomodulin in each group were detected with fluorescence microscope (IX71, Olympus) after co-culture for 14 days. After being treated with 4% paraformaldehyde, the samples were blocked with 4% BSA and were incubated with primary antibody (Sox-9: bs-4177R, Bioss; Tenomodulin: bs-7525R, Bioss, Woburn, MA, USA) at 4°C overnight. Then, the samples were treated with the secondary Anti-Rabbit IgG (ab150075, Abcam, Cambridge, UK) at room temperature for 1 h. Subsequently, DAPI was added. Three visions were selected randomly for each sample, and total 24 visions were measured for each group of eight samples.

Macrophage polarisation and release of inflammatory factors at the bone–tendon healing interface were observed by immunofluorescence staining. Briefly, paraffin sections were dewaxed and subjected to a graded alcohol series and distilled water. For antigen retrieval, tissue sections were incubated with trypsin at 37°C for 30 min, placed in sodium borohydride solution at room temperature for 30 min and blocked with 4% BSA for 1 h. After incubation at 4°C overnight with primary antibody (CD206: bs-2664R, Bioss; IL-10: bs-0698R, Bioss) diluted in 0.01 mol/L phosphate buffered saline (PBS), sections were incubated with secondary Anti-Rabbit IgG (ab150075, Abcam) at room temperature for 1 h, followed by DAPI counterstained. Three visions were selected randomly for each sample, and total 18 visions were measured (n = 6).

The preparation of MSCS and seeding of MSCS onto ATS

MSCs were cultured at 1 × 104 cells/cm2 on temperature-responsive culture dish (Thermo Fisher Scientific, Waltham, MA, USA) at 37°C. After about 1 week, MSCS was formed by placing the culture dish at room temperature for about 30 min. Then MSCSs were set on each layer of the sterilised book-shaped ATS. Fig. 1 shows the diagrammatic drawing of the preparation of MSCSs and seeding of MSCSs onto ATS.

Establishment of partial patellectomy model and grouping

A total of 144 male or female rabbits which weigh 3.0 ± 0.5 kg (18-weeks-old) were used for partial patellectomy at a previous protocol [30]. After being treated with sodium pentobarbital (3%) for narcosis, the transverse osteotomy was performed between the distal 1/3 and the proximal 2/3 of the patella. After removing the distal 1/3 of the patella and the fibrocartilage tissue, two holes (diameter, 0.8 mm) were perforated parallelly through the residual patella, then the residual patella and the patellar tendon were reattached with 3-0 polydioxanone suture (Ethicon, Bridgewater, NJ, USA). A figure-of-8 tension band wire was applied from the superior pole of the residual patella to the tibial tuberosity to enhance the reattachment at the junction. The knee was immobilised with plaster and bandage after surgery.

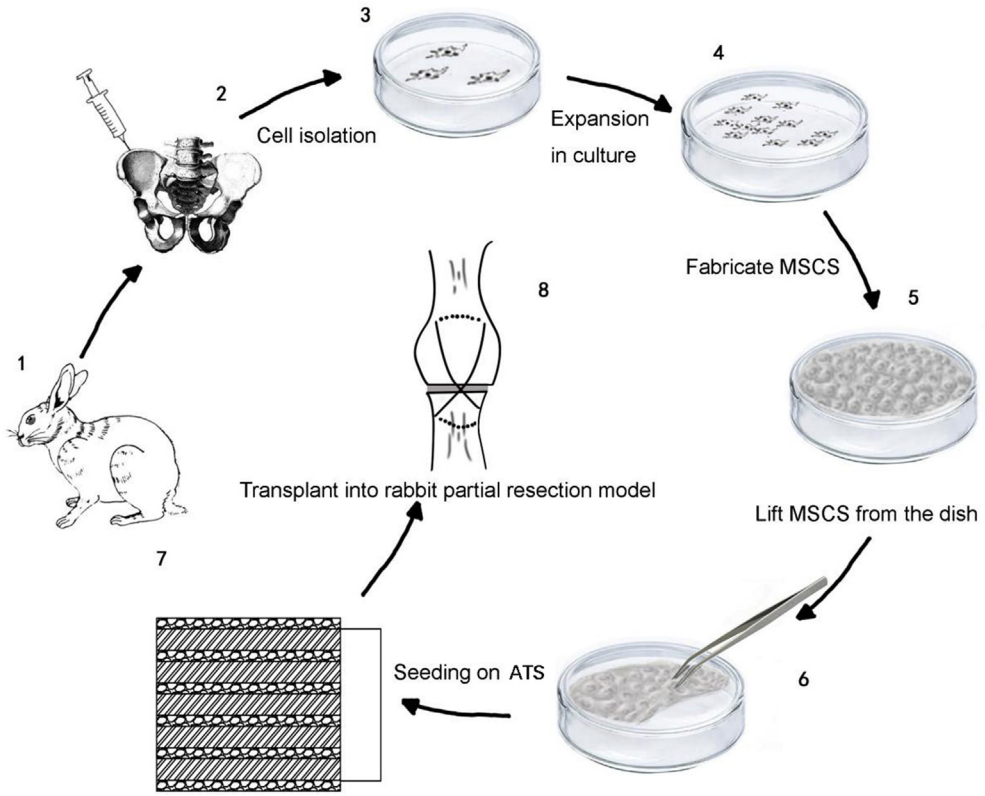

Figure 1. The diagrammatic drawing of the preparation of MSCS and the combination of MSCS and ATS. ATS = acellular tendon scaffold; MSCS = mesenchymal stem cells sheet.

The experiment was divided into three groups: (1) control group: partial patellotomy with nothing implanted; (2) ATS group: ATS was implanted between residual patella and patellar tendon and (3) ATS + MSCS group: the complex of ATS and MSCS was implanted between residual patella and patellar tendon.

All experimental procedures about animals were approved by the Ethics Committee of the Center for Scientific Research with Animal Models of Central South University (2014-3-12).

Tissue samples preparation

The PPT complex samples were collected after postoperative week 2, 4, 8 and 16, respectively. The samples for histological evaluation were decalcified with 0.5 M ethylene diamine tetraacetic acid (EDTA) (Sigma–Aldrich, USA) for 90 days (n = 6 for each group). Then samples were paraffin-embedded and cut into the thickness of 5 μm sections. Samples for biomechanical testing were placed at −80°C (n = 6 for each group).

Histological analysis

Section was stained with H&E for the evaluation of new bone and with toluidine blue to evaluate the regenerated fibrocartilage. The area of regenerated bone and the thickness of the newly formed fibrocartilage zone were calculated by a previously established protocol [30–32].

Mechanical analysis

The mechanical property was evaluated by a biomechanical testing machine (MTS Insight, Eden Prairie, MN, USA), including the failure load, energy at failure and ultimate tensile strength. Before testing, the samples were thawed overnight at 4°C, then the soft tissue, suture, band wire around the PPT were carefully dissected. The width and thickness of the PPT were measured by a caliper under a constant tensile load (5 N), and the operation was repeated three times, and the average value was used to calculate the area of the PPT. The failure load was tested at a rate of 20 mm/min after a preload of 1 N. The failure load divided by the area of the PPT was the ultimate tensile strength.

Statistical analysis

All data were expressed as mean ± standard deviation and were analysed by SPSS 25.0 software. Two-way analysis of variance was used to compare the effect of stem cell or scaffold and healing time on the regeneration of damaged tissue, with Bonferroni post hoc test for statistical differences. A $p < 0.05$ indicates statistically significant difference.

Results

Characterisation of ATS

The gross observation of the scaffold (7 mm × 2 mm × 1 mm) was shown in Fig. 2A. H&E staining of the scaffold showed that the native collagen structure of the acellular scaffold was preserved without any residual of cellular components (Fig. 2B), and DAPI staining results demonstrated that there was almost no cell observed after decellularisation (Fig. 2C). The microstructure of the scaffold before and after decellularisation was observed by SEM. Before decellularisation, the cellular components were observed, whereas after decellularisation, absolutely no cellular components were remained on the tendon fibres, and the native collagen structure was preserved (Fig. 2D).

Differentiation inductivity of ATS

Gene expression profiles of MSCs seeded on ATS at 7 days and 14 days were analysed by qRT-PCR. The expression levels of tenomodulin, alpha-

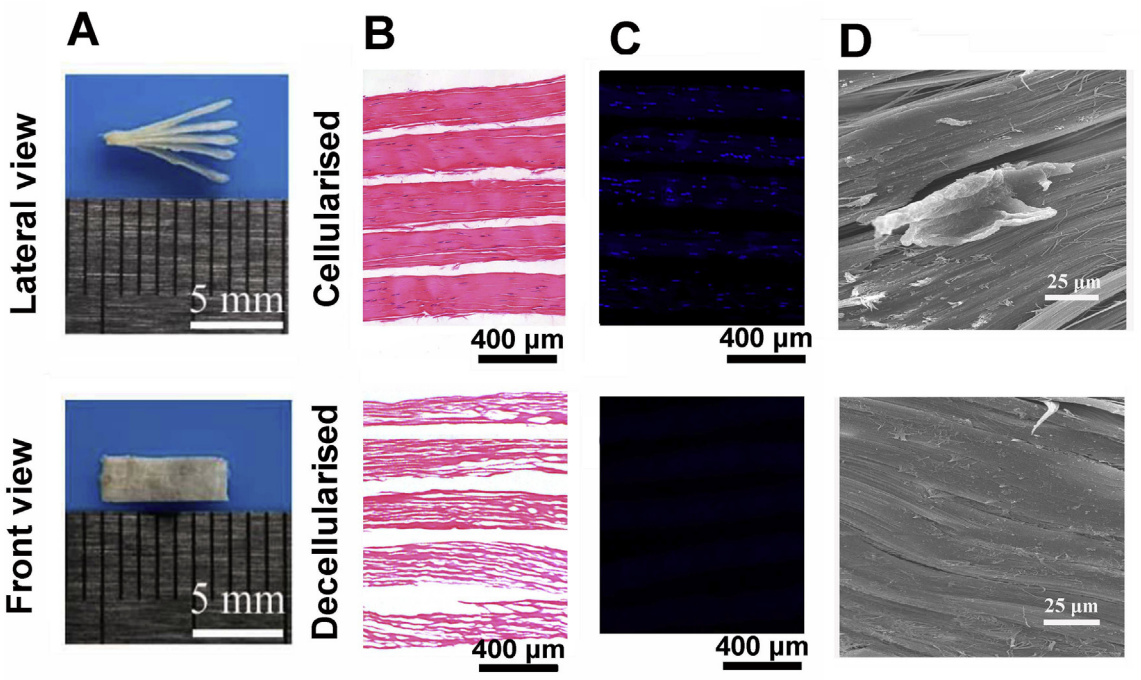

Figure 2. (A) Macroscopic features of the book-shaped acellular tendon scaffold; (B) H&E staining of the native and acellular book-shaped tendon scaffold; (C) DAPI staining of the native and acellular book-shaped tendon scaffold; (D) SEM observation of the native and acellular book-shaped tendon scaffold. H&E = haematoxylin and eosin; DAPI, 4',6-diamidino-2-phenylindole; SEM = scanning electron microscope.

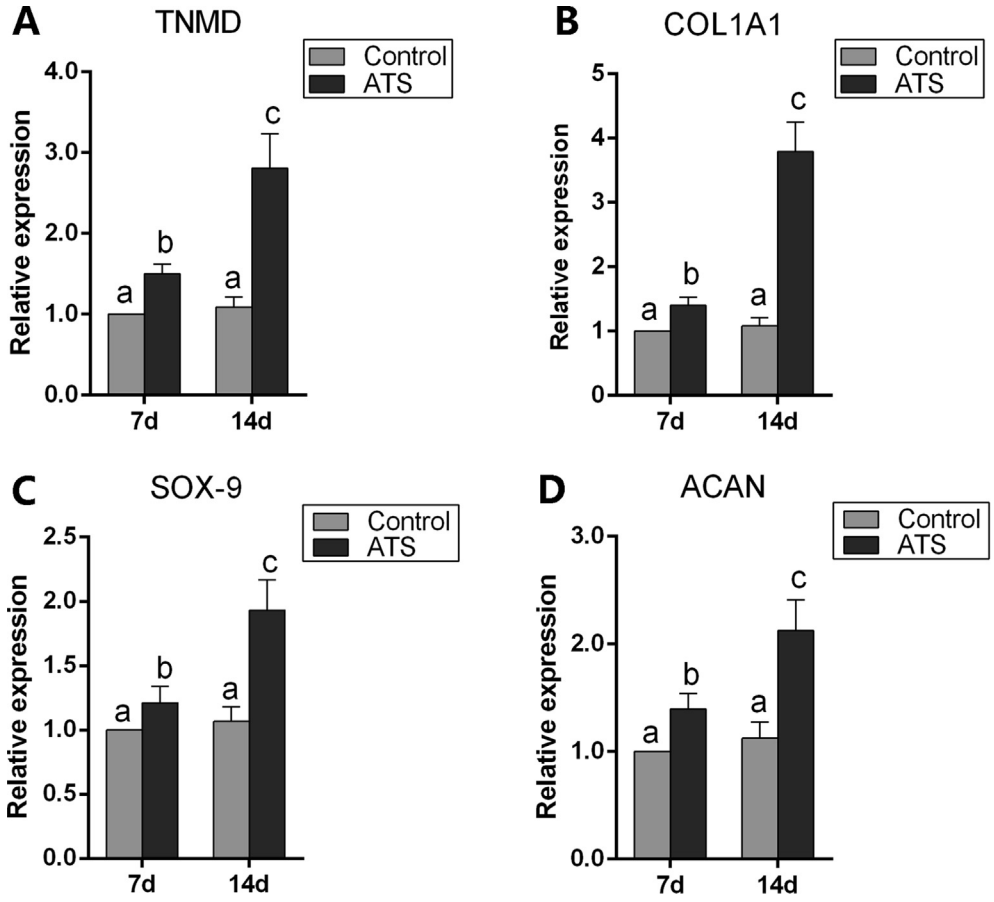

Figure 3. (A,B) Analysis of gene expression involving tenogenic differentiation; (C, D) analysis of gene expression involving chondrogenic differentiation. Different letters represent statistical significant difference, $p < 0.05$. ATS = acellular tendon scaffold; TNMD = Tenomodulin; ACAN = Aggrecan.

1 type I collagen, Sox-9 and aggrecan in the ATS group all up-regulated compared with the control group at 7 days and 14 days ($p < 0.05$), and expression of above genes were also upregulated from day 7 to day 14 in the ATS group ($p < 0.05$) (Fig. 3A–D).

On analysing the expression of tenomodulin and Sox-9 by IF, the amount of cells positive for tenomodulin in the ATS group (158 ± 44/mm^2) was higher than the control group significantly (0/mm^2) ($p < 0.05$). And the amount of cells positive for Sox-9 in the ATS group (114 ± 46/mm^2) was also higher than the control group significantly (0/mm^2) ($p < 0.05$) (Supplementary Fig. 1).

Histomorphometric analysis of repaired PPT

After 4, 8 and 16 weeks postoperation, the repaired PPT were obtained for histomorphometric evaluation. At 8 weeks postoperatively, new bone could be observed at the regenerated PPT in all groups, but much more regenerated bone was shown in the ATS+MSCS group than other groups ($p < 0.05$). At 16 weeks postoperatively, there was more regenerated bone in the ATS + MSCS group than other groups ($p < 0.05$), and there was also statistical difference between the ATS group and control group ($p < 0.05$) (Fig. 4).

Meanwhile, the regeneration of fibrocartilage layer was analysed. At 8 weeks postoperatively, fibrocartilage layer could be seen at the regenerated PPT interface in all groups. The thickness of fibrocartilage layer between the control group (0.30 ± 0.03 mm) and the ATS group (0.32 ± 0.04 mm) did not show a statistical difference ($p > 0.05$). However, the specimens in the ATS+MSCS group (0.52 ± 0.07 mm) showed a significantly thicker fibrocartilage layer than other groups ($p < 0.05$). At 16 weeks after surgery, the thickness of the fibrocartilage layer among the ATS+MSCS group, the ATS group and the control group was 0.98 ± 0.07 mm, 0.88 ± 0.06 mm and 0.77 ± 0.06 mm, respectively, and pairwise comparisons between groups also showed a statistical difference ($p < 0.05$) (Fig. 5).

Effect of ATS and MSCS on macrophage polarisation toward the M2 phenotype and IL-10 expression

Considering the potential of the ATS and MSCS to modulate macrophage polarisation, we examined the expression of M2 marker CD206 by immunofluorescence (IF) staining, and the amount of CD206$^+$

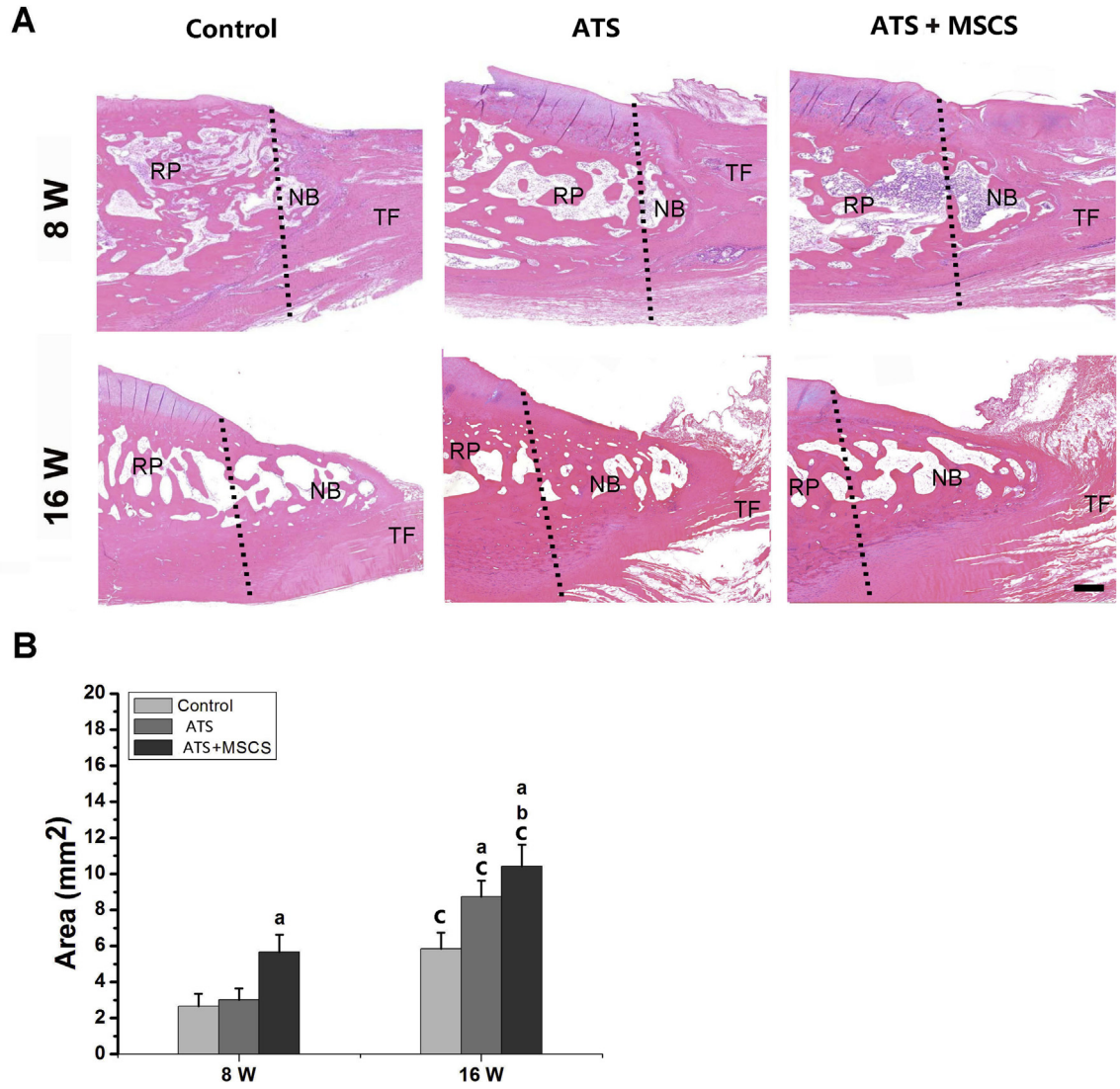

Figure 4. The area of new bone of regenerated patella–patellar tendon interface at 8 and 16 weeks postoperatively: (A) Representative H&E staining images; (B) semiquantitative analysis of the area of new bone. Scale bars = 100 μm. [a]Significantly different from the control group at the same time point postoperatively, $p < 0.05$; [b]Statistically significant difference between the ATS group and the ATS+ MSCS group at the same time point postoperatively, $p < 0.05$; [c]Statistical difference between 8 and 16 weeks postoperatively in the same group, $p < 0.05$. The dotted line shows the osteotomy site. ATS = acellular tendon scaffold; MSCS = mesenchymal stem cells sheet; NB = newly formed bone; RP = remaining patella; TF = tendon fibre.

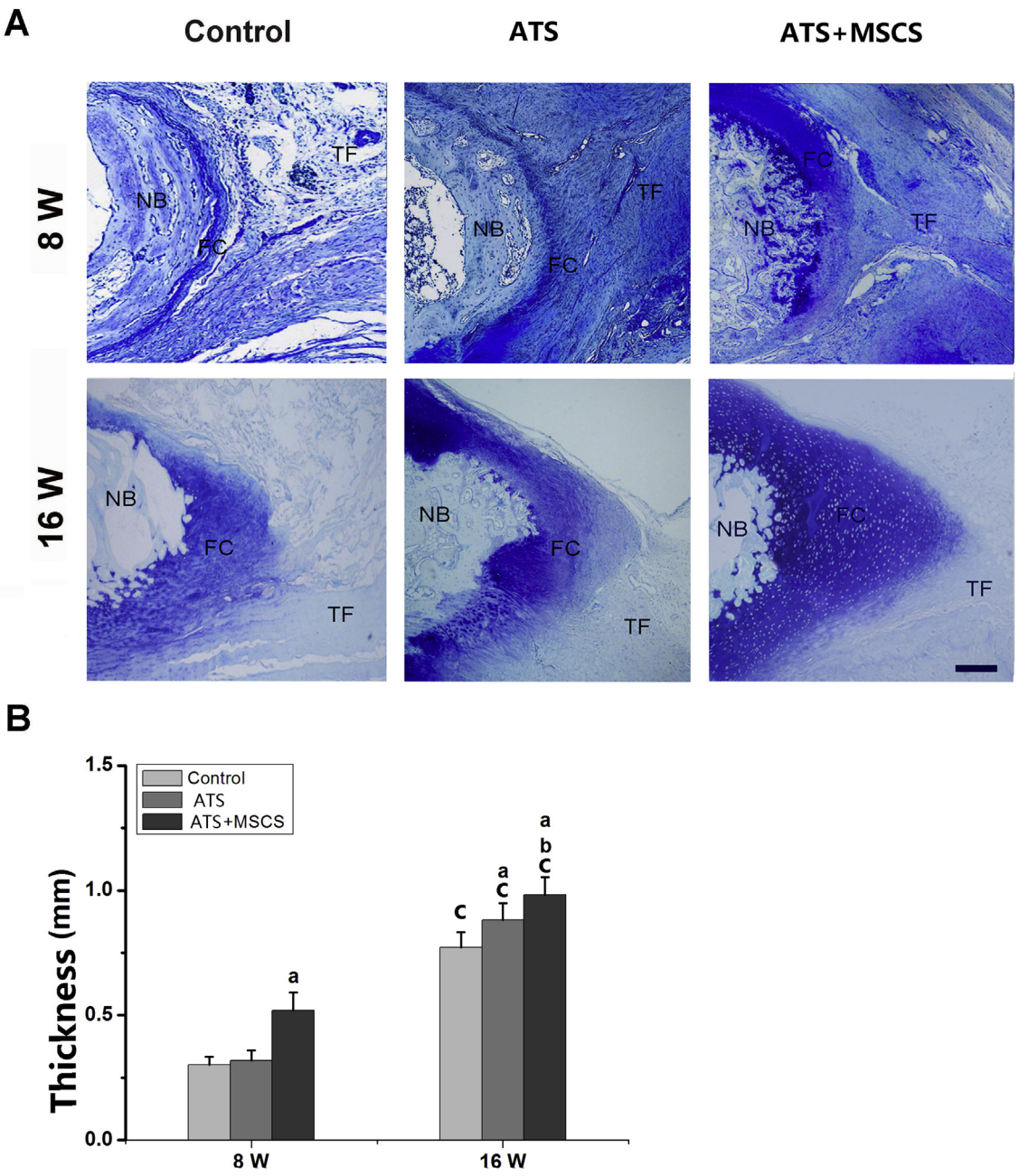

Figure 5. The regenerated fibrocartilage of regenerated patella–patellar tendon interface at 8 and 16 weeks postoperatively: (A) Representative toluidine blue staining images; (B) semiquantitative analysis of the thickness of the regenerated fibrocartilage layer. Scale bars = 600 μm [a]Significantly different from the control group at the same time point postoperatively, $p < 0.05$; [b]Statistical difference between the ATS group and the ATS+ MSCS group at the same time point postoperatively, $p < 0.05$; [c]Statistical difference between 8 and 16 weeks postoperatively in the same group, $p < 0.05$. ATS, acellular tendon scaffold; FC, fibrocartilage; MSCS, mesenchymal stem cells sheet; NB = newly formed bone; TF = tendon fibre.

cells were calculated by positive nuclear staining. The results showed the gradually increased amount of CD206$^+$ macrophages from week 2 to 8 postoperatively in each group, whereas there was no statistical difference between 8 and 16 weeks postoperatively. Moreover, the number of CD206$^+$ macrophages in the control group was significantly lower than other groups at 4, 8 and 16 weeks postoperatively ($p < 0.05$), and the number of CD206$^+$ macrophages in the ATS + MSCS group was also significantly higher than that in the ATS group at week 8 and 16 after surgery ($p < 0.05$). There is no significant difference among the groups at 2 weeks after surgery (Fig. 6).

Meanwhile, there was an increasing trend of the expression of interleukin (IL)-10$^+$ cells from 4 to 8 weeks postoperatively but decreasing from postoperative week 8–16. The amount of IL-10$^+$ cells in the ATS+MSCS group was higher than other groups significantly at 4 and 8 weeks postoperatively ($p < 0.05$). Moreover, the difference was also statistical difference between the ATS and the control groups at 8 weeks after surgery ($p < 0.05$), but there was no statistical difference among groups at 16 weeks postoperatively ($p > 0.05$) (Supplementary Fig. 2).

Biomechanical analysis

Mechanical testing results indicated that the biomechanical property of the regenerated PPT were greatly advanced with healing time and improved with the implantation of ATS and MSCS (Table 2). At postoperative week 8 and 16, the failure load, energy at failure, and ultimate tensile strength in the ATS+MSCS group were significantly higher than

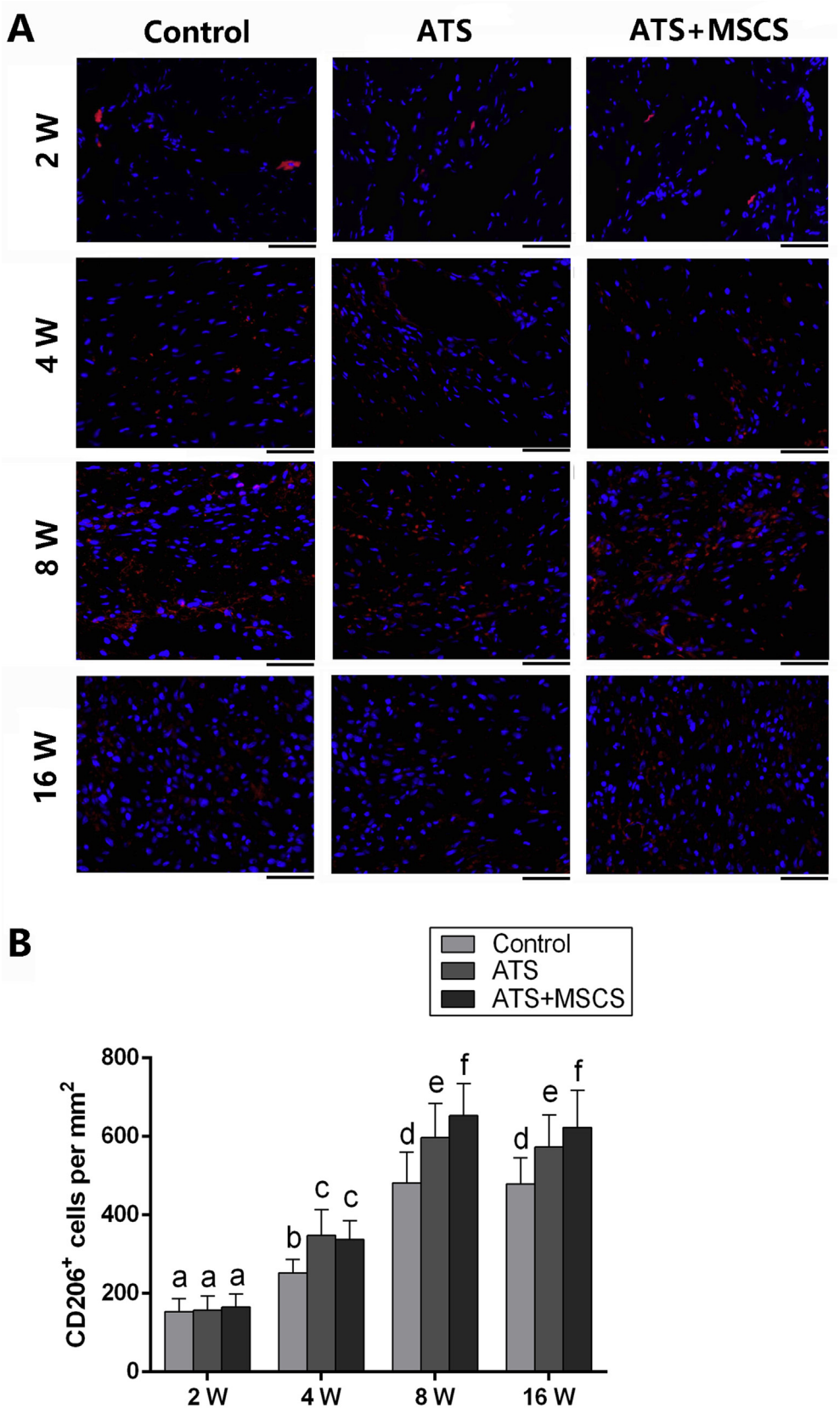

Figure 6. The expression of CD206 at regenerated patella–patellar tendon interface at 2, 4, 8 and 16 weeks postoperatively: (A) IF staining images of representative CD206^{+} macrophages; (B) semiquantitative analysis of CD206+ macrophages. Scale bars = 45 μm. Different letters represent statistical significance, $p < 0.05$. ATS = acellular tendon scaffold; MSCS = mesenchymal stem cells sheet.

Table 2
Biomechanical properties of the patella–patellar tendon interface.

Test item	8W			16W		
	Control group	ATS group	ATS+MSCS group	Control group	ATS group	ATS+MSCS group
Failure Load(N)	152.62 ± 16.21	193.18 ± 9.41[a]	229.54 ± 9.65[b,c]	249.38 ± 10.14[d]	308.25 ± 22.59[a,d]	389.5 ± 20.47[b,c,d]
Ultimate Strength (Mpa)	3.81 ± 0.82	6.21 ± 0.43[a]	7.86 ± 0.38[b,c]	5.22 ± 0.42[d]	7.31 ± 0.75[a,d]	10.33 ± 0.87[b,c,d]
Energy at Failure(J)	0.27 ± 0.02	0.35 ± 0.03[a]	0.47 ± 0.02[b,c]	0.61 ± 0.03[d]	0.78 ± 0.04[a,d]	0.95 ± 0.03[b,c,d]

ATS = acellular tendon scaffold; MSCS = mesenchymal stem cells sheet.
[a] Statistical difference between the ATS group and the control group at the same time point postoperatively, $p < 0.05$.
[b] Statistical difference between the ATS+MSCS group and the control group at the same time point postoperatively, $p < 0.05$.
[c] Statistical difference between the ATS+MSCS group and the ATS group at the same time point postoperatively, $p < 0.05$.
[d] Statistical difference between 8 and 16 weeks postoperatively in the same group, $p < 0.05$.

other groups ($p < 0.05$), and there was also significant difference between the ATS group and the control group ($p < 0.05$). Furthermore, from week 8 to 16 postsurgery, the biomechanical properties advanced in the same group. All samples failed at the place between the residual patella and the regenerated bone, and all samples were tested at the same condition and parameter.

Discussion

BTI injury is common in clinical, but the surgery on it often has a high failure rate [8–10], because of the slow and difficult regeneration of the fibrocartilage layer [4–7]. Under the above circumstances, the development of tissue engineering has promoted the BTI healing. In this study, rabbit Achilles tendon as a substrate was removed cells to prepare a book-shaped ATS. To enrich the biological property of the ATS, MSCs were seeded on ATS, and the differentiation profiles of MSCs were also investigated. Tenomodulin, alpha-1 collagen type I, Sox-9 and Aggrecan are important indicators for evaluating MSCs differentiating into tendon and cartilage. When MSCs were co-cultured with ATS for 7 and 14 days, both qRT-PCR and IF staining results showed that MSCs express the relevant markers, which indicated that ATS can induce MSCs to differentiate into tendon and cartilage. The possible mechanism is that the morphological and chemical structure of the scaffold is similar to that of the native tendon, which has induced the differentiation of MSCs [16,17]. Another possible mechanism is the similar biomechanical properties between ATS and the autologous tendons and appropriate biomechanical stimulation can facilitate the differentiation of stem cells [18]. In previous studies, the decellularised scaffold has the characteristics of high density and low porosity, the implanted cells are usually confined to the surface of the scaffold and it takes a long time to migrate into the interior of the acellular scaffold [33–35]. Different from it, the novel book-shaped scaffold designed in our study not only has the advantages of traditional biomaterials, which has low immunogenicity and stem cell differentiation inductivity, but also is easy for decellularisation and cell plant.

Effective repair of fibrocartilage is the key issue for BTI injury repair. In prior studies, the tissue-engineered scaffolds for bone tendon healing are often synthetic and natural biomaterials. For example, Tien et al. developed the calcium-phosphate cement, which can promote the augmentation of tendon–bone healing [11]. Moreover, Mutsuzaki et al. prepared the calcium phosphate-hybridised tendon graft, which can be used for the anterior cruciate ligament reconstruction [13]. However, the regeneration of BTI still remained a challenge because of the low bioactivity of the above biomaterials. Therefore, to overcome these shortcomings, a composite containing MSCS and the book-shaped ATS was applied to the rabbit partial patellotomy model in the current study. H&E and toluidine blue staining results in this study indicated that ATS combined with MSCS could effectively promote the regeneration of bone and cartilage at the PPT interface. Meanwhile, biomechanical analysis showed that ATS combined with MSCS can effectively enhance the biomechanical property of the PPT. Possible explanations for this enhancement may be related to the chondrogenic differentiation of MSCs induced by ATS, which need to be further studied.

In *in vivo* study, we also observed the effect of the complex on the regulation of local immune microenvironment in tendon to bone interface. The polarisation of macrophages plays a significant role in the remodelling process after tissue injury [36]. M2 macrophages can reduce inflammation and promote tissue regeneration [37,38]. Studies by Sicari et al. have shown that ECM from small intestine submucosa can promote macrophage polarisation to M2 [39]. Other studies have showed that coating dermal-derived ECM hydrogel onto polypropylene mesh can polarise macrophages towards the M2 phenotype [40]. Related parallel studies have shown that adipose MSCs can secrete antiinflammatory cytokines that promote macrophages polarisation to M2 [41]. Our results are consistent with above results. IF staining showed that ATS can stimulate local macrophages polarisation to M2 in healing process at PPT interface. MSCs has no obvious influence on macrophage polarisation towards M2 in the early healing stage but produced significant effect on macrophage polarisation in the late healing stage. Meanwhile, both ATS and MSCS promoted the expression of IL-10. Therefore, we believe that ATS and MSCS can regulate the local immune inflammatory microenvironment at the PPT interface.

In conclusion, ATS can provide physical structure and chemical component for MSCs to differentiate into cartilage and tendon. ATS combined with MSCS can regulate inflammatory microenvironment and promote fibrocartilage regeneration, thus promoting the healing of PPT interface. The limitation of this study is that the MSCs were not labelled to track the fate of transplanted cells. It was unknown whether the transplanted cells survived in the healing zone. The host chondrocytes, MSCs that were recruited to the defect margins or MSCs sheets implanted may play a crucial role in fibrocartilage reconstruction. Moreover, transplanted MSCs were not autologous, which may lead to immune rejection to some extent.

Authors' contributions

H.L. and J.H. conceived and designed the research. Y.Z. and S.X. completed the experiments. Y.T., X.L. and Y.C. analysed the data. Y.Z. and S.X. wrote the paper. The authors declare that they have read and approved submitting the manuscript.

Conflicts of Interest

The authors have no conflicts of interest to disclose in relation to this article.

Acknowledgements

This work was supported by National Key R&D Program of China (No. 2018YFC1105104), National Natural Science Foundation of China (No. 81730068 and No. 81472072) and China Postdoctoral Science Foundation (No. 2017M622613).

The authors would like to thank professor Hui Xie and other staff from Movement System Injury and Repair Research Center, Xiangya Hospital,

Central South University, Changsha, China, for their kind assistance during the experiments.

Appendix A. Supplementary data

Supplementary data to this article can be found online at https://doi.org/10.1016/j.jot.2020.02.013.

References

[1] Leung KS, Qin L, Fu LK, Chan CW. A comparative study of bone to bone repair and bone to tendon healing in patella-patellar tendon complex in rabbits. Clin Biomech (Bristol, Avon) 2002;17(8):594–602.

[2] Lu H, Liu F, Chen H, Chen C, Qu J, Xu D, et al. The effect of low-intensity pulsed ultrasound on bone-tendon junction healing: initiating after inflammation stage. J Orthop Res 2016;34:1697–706.

[3] Benjamin M, McGonagle D. Entheses: tendon and ligament attachment sites. Scand J Med Sci Sports 2006;19:520–7.

[4] Leung KS, Chong WS, Chow DH, Zhang P, Cheung WH, Wong MW, et al. A comparative study on the biomechanical and histological properties of bone-to-bone, bone-to-tendon, and tendon-to-tendon healing: an Achilles tendon-calcaneus model in goats. Am J Sports Med 2015;43(6):1413–21.

[5] Lu H, Chen C, Qu J, CheEn H, Chen Y, Zheng C, et al. Initiation timing of low-intensity pulsed ultrasound stimulation for tendon-bone healing in a rabbit model. Am J Sports Med 2016;44(10):2706–15.

[6] Xu D, Zhang T, Qu J, Hu J, Lu H. Enhanced patella-patellar tendon healing using combined magnetic fields in a rabbit model. Am J Sports Med 2014;42(10):2495–501.

[7] Hu J, Qu J, Xu D, Zhang T, Qin L, Lu H. Combined application of low-intensity pulsed ultrasound and functional electrical stimulation accelerates bone-tendon junction healing in a rabbit model. J Orthop Res 2014;32(2):204–9.

[8] Deprés-Tremblay G, Chevrier A, Snow M, Hurtig MB, Rodeo S, Buschmann MD. Rotator cuff repair: a review of surgical techniques, animal models, and new technologies under development. J Shoulder Elbow Surg 2016;25(12):2078–85.

[9] Lichtenberg S, Liem D, Magosch P, Habermeyer P. Influence of tendon healing after arthroscopic rotator cuff repair on clinical outcome using single-row Mason-Allen suture technique: a prospective, MRI controlled study. Knee Surg Sports Traumatol Arthrosc 2006;14(11):1200–6.

[10] Colvin AC, Egorova N, Harrison AK, Moskowitz A, Flatow EL. National trends in rotator cuff repair. J Bone Joint Surg Am 2012;94(3):227–33.

[11] Tien YC, Chih TT, Lin JH, Ju CP, Lin SD. Augmentation of tendon-bone healing by the use of calcium-phosphate cement. J Bone Joint Surg Br 2004;86:1072–6.

[12] Zhao C, Sun YL, Zobitz ME, An KN, Amadio PC. Enhancing the strength of the tendon-suture interface using 1-ethyl-3-(3-dimethylaminopropyl) carbodiimide hydrochloride and cyanoacrylate. J Hand Surg Am 2007;32:606–11.

[13] Mutsuzaki H, Kanamori A, Ikeda K, Hioki S, Kinugasa T, Sakane M. Effect of calcium phosphate-hybridized tendon graft in anterior cruciate ligament reconstruction: a randomized controlled trial. Am J Sports Med 2012;40:1772–80.

[14] Ouyang HW, Goh JC, Lee EH. Use of bone marrow stromal cells for tendon graft-to-bone healing: histological and immunohistochemical studies in a rabbit model. Am J Sports Med 2004;32:321–7.

[15] Soon MY, Hassan A, Hui JH, Goh JC, Lee EH. An analysis of soft tissue allograft anterior cruciate ligament reconstruction in a rabbit model: a short-term study of the use of mesenchymal stem cells to enhance tendon osteointegration. Am J Sports Med 2007;35:962–71.

[16] Keane TJ, Swinehart IT, Badylak SF. Methods of tissue decellularization used for preparation of biologic scaffolds and in vivo relevance. Methods 2015;84:25–34.

[17] Guo L, Qu J, Zheng C, Cao Y, Zhang T, Lu H, et al. Preparation and characterization of a novel decellularized fibrocartilage "book" scaffold for use in tissue engineering. PloS One 2015;10(12). e0144240.

[18] Goktas S, Pierre N, Abe K, Dmytryk J, McFetridge PS. Cellular interactions and biomechanical properties of a unique vascular-derived scaffold for periodontal tissue regeneration. Tissue Eng Part A 2010;16(3):769–80.

[19] Tan QW, Zhang Y, Luo JC, Zhang D, Xiong BJ, Yang JQ, et al. Hydrogel derived from decellularized porcine adipose tissue as a promising biomaterial for soft tissue augmentation. J Biomed Mater Res A 2017;105(6):1756–64.

[20] Kishore Vipuil, Bullock Whitney, Sun Xuanhao, Van Dyke William Scott, Akkus Ozan. Tenogenic differentiation of human MSCs induced by the topography of electrochemically aligned collagen threads. Biomaterials 2012;33(7):2137–44.

[21] Xie J, Peng C, Zhao Q, Wang X, Yuan H, Yang L, et al. Osteogenic differentiation and bone regeneration of iPSC-MSCs supported by a biomimetic nanofibrous scaffold. Acta Biomater 2016;29:365–79.

[22] Li Q, Gao Z, Chen Y, Guan MX. The role of mitochondria in osteogenic, adipogenic and chondrogenic differentiation of mesenchymal stem cells. Protein Cell 2017;8(6):439–45.

[23] Mitani G, Sato M, Lee JI, Kaneshiro N, Ishihara M, Ota N, et al. The properties of bioengineering chondrocyte sheets for cartilage regeneration. BMC Biotechnol 2009;9:17.

[24] Kobayashi T, Kan K, Nishida K, Yamato M, Okano T. Corneal regeneration by transplantation of corneal epithelial cell sheets fabricated with automated cell culture system in rabbit model. Biomaterials 2013;34:9010–7.

[25] Lin YC, Grahovac T, Oh SJ, Ieraci M, Rubin JP, Marra KG. Evaluation of a multi-layer adipose-derived stem cell sheet in a full-thickness wound healing model. Acta Biomater 2013;9:5243–50.

[26] Long T, Zhu Z, Awad HA, Schwarz EM, Hilton MJ, Dong Y. The effect of mesenchymal stem cell sheets on structural allograft healing of critical sized femoral defects in mice. Biomaterials 2014;35:2752–9.

[27] You Q, Liu Z, Zhang J, Shen M, Li Y, Jin Y, et al. Human amniotic mesenchymal stem cell sheets encapsulating cartilage particles facilitate repair of rabbit osteochondral defects. Am J Sports Med 2020;48(3):599–611.

[28] Onizuka S, Iwata T. Application of periodontal ligament-derived multipotent mesenchymal stromal cell sheets for periodontal regeneration. Int J Mol Sci 2019;20(11). pii: E2796.

[29] Hu J, Zhou Y, Huang L, Jun L, Lu H. Effect of nano-hydroxyapatite coating on the osteoinductivity of porous biphasic calcium phosphate ceramics. BMC Muscoskel Disord 2014;15:114.

[30] Lu H, Qin L, Cheung W, Lee K, Wong W, Leung K. Low-intensity pulsed ultrasound accelerated bone-tendon junction healing through regulation of vascular endothelial growth factor expression and cartilage formation. Ultrasound Med Biol 2008;34(8):1248–60.

[31] Wang W, Chen HH, Yang XH, Xu G, Chan KM, Qin L. Postoperative programmed muscle tension augmented osteotendinous junction repair. Int J Sports Med 2007;28(8):691–6.

[32] Lu H, Chen C, Qu J, Chen H, Chen Y, Zheng C, et al. Initiation timing of low-intensity pulsed ultrasound stimulation for tendon-bone healing in a rabbit model. Am J Sports Med 2016;44(10):2706–15.

[33] Crapo PM, Gilbert TW, Badylak SF. An overview of tissue and whole organ decellularization processes. Biomaterials 2011;32:3233–43.

[34] Woon CY, Farnebo S, Schmitt T, Kraus A, Megerle K, Pham H, et al. Human flexor tendon tissue engineering: revitalization of biostatic allograft scaffolds. Tissue Eng Part A 2012;18(23–24):2406–17.

[35] Ozasa Y, Amadio PC, Thoreson AR, An KN, Zhao C. Repopulation of intrasynovial flexor tendon allograft with bone marrow stromal cells: an ex vivo model. Tissue Eng Part A 2014;20(3–4):566–74.

[36] Novak ML, Koh TJ. Phenotypic transitions of macrophages orchestrate tissue repair. Am J Pathol 2013;183:1352–63.

[37] Deng B, Wehling-Henricks M, Villalta SA, Wang Y, Tidball JG. IL-10 triggers changes in macrophage phenotype that promote muscle growth and regeneration. J Immunol 2012;189:3669–80.

[38] Wynn TA, Vannella KM. Macrophages in tissue repair, regeneration, and fibrosis. Immunity 2016;44(3):450–62.

[39] Sicari BM, Dziki JL, Siu BF, Medberry CJ, Dearth CL, Badylak SF. The promotion of a constructive macrophage phenotype by solubilized extracellular matrix. Biomaterials 2014;35(30):8605–12.

[40] Wolf MT, Dearth CL, Ranallo CA, LoPresti ST, Carey LE, Daly KA, et al. Macrophage polarization in response to ECM coated polypropylene mesh. Biomaterials 2014;35(25):6838–49.

[41] Gonzalez-Rey E, Gonzalez MA, Varela N, O'Valle F, HErnandez-Cortes P, Rico L, et al. Human adipose-derived mesenchymal stem cells reduce inflammatory and T cell responses and induce regulatory T cells in vitro in rheumatoid arthritis. Ann Rheum Dis 2010;69(1):241–8.